

Pattern Formation on Networks with Reactions: A Continuous Time Random Walk Approach

C. N. Angstmann,^{*} I. C. Donnelly,[†] and B. I. Henry[‡]

School of Mathematics and Statistics,

University of New South Wales, Sydney, NSW 2052, Australia

(Dated: August 28, 2022)

Abstract

We derive the generalised master equation for reaction-diffusion on networks from an underlying stochastic process, the continuous time random walk (CTRW). Using this model we have investigated different types of pattern formation across the vertices on a range of networks. Importantly, the CTRW defines the Laplacian operator on the network in a non ad-hoc manner and the pattern formation depends on the structure of this Laplacian. Here we focus attention on CTRWs with exponential waiting times for two cases; one in which where the rate parameter is constant for all vertices and the other where the rate parameter is proportional to the vertex degree. This results in non-symmetric and symmetric CTRW Laplacians respectively. In the case of symmetric Laplacians, pattern formation follows from the Turing instability. However in non-symmetric Laplacians, pattern formation may be possible with or without a Turing instability.

^{*} c.angstmann@unsw.edu.au

[†] i.donnelly@unsw.edu.au

[‡] b.henry@unsw.edu.au

I. INTRODUCTION

Networks have been extensively studied as models for highly connected systems in biology [1], physics [2] and the social sciences [3]. Here we consider the dynamics of reaction-diffusion networks with reactions of particles on vertices and diffusion of particles between vertices. One of the interesting features of these systems is the possibility of spontaneous pattern formation whereby the concentration of particles is non-homogeneously distributed across the network.

Reaction-diffusion models form the basis of pattern formation in a wide range of self-organising systems. Turing's seminal work in 1952 [4] showed that in a two species system with reaction and diffusion, patterns may arise (Turing patterns) due to an instability in the reaction dynamics caused by differing rates of diffusion. Such patterns emerge in biological morphogenesis [5–9] chemical reactions [10], propagation of viruses [11, 12] as well as ecosystems encompassing competing animals [13].

In early work, the existence of Turing patterns on networks was explored by Othmer and Scriven [14] whereby they showed that the structure of the network has a direct effect on the resulting pattern. Similar behaviour was also reported by Colizza et. al. [15]. Subsequent studies have considered scale-free networks [16], coupled reactors [17] and functional gene networks [18].

Recent studies of reaction and diffusion on networks have identified that multiple coexisting stationary states exist for many systems [19–22]. The effects of feedback [20] and the formation of travelling fronts [22] have also been studied in these systems.

A discrete space description of diffusion can be modelled by a Random Walk (RW) [23–25]. RW on networks have been extensively studied in this context. See for example [26–28].

The continuous time random walk (CTRW) is a generalization of the random walk in which the random walker waits a time (drawn from a waiting time probability density) before jumping [29, 30]. This model has been particularly useful to model diffusion in systems with disorder in waiting times resulting in anomalous diffusion [31]. The continuous time random walk has been further generalized to include linear reactions [32, 33], linear reactions with multiple species [34] and nonlinear reactions [35–39].

Continuous time random walks on networks without reactions have been studied in [40]. Here we consider continuous time random walks with reactions on networks. The descrip-

tion is at the mesoscopic level, with particles jumping between vertices and with reactions between particles at vertices. This model description could be applied to the analysis of diffusion tensor imaging data [41, 42] and to spatio-temporal models in epidemiology [43, 44]. The essential assumption in this description is that there is an underlying stochastic process that defines the motion of particles on the network that may be modelled as a CTRW. Specifically, we assume that each vertex in the network can be occupied by any number of walkers and the reactions among the walkers at a vertex are governed by the same reaction kinetics at all vertices. Our principal concern is then the collective motion of the walkers on the network as a whole.

Within this CTRW framework we have derived a family of diffusive network Laplacian operators. The reaction-diffusion behaviour with these network Laplacian operators may differ from that with the continuum Laplacian operator [45]. In the following we have considered pattern formation arising from continuous time random walks on networks with reactions using the different forms of the Laplacian.

The remainder of the paper is as follows. In section II we derive the master equations that describe the continuous time random walk network reaction diffusion model. In section III we describe different pattern formation mechanisms that may arise depending on the form of the CTRW Laplacian. In section IV we present numerical simulations of pattern formation in the network models. We conclude with a summary and discussion in section V

II. DERIVATION OF A CTRW NETWORK REACTION DIFFUSION MASTER EQUATIONS

Diffusion, or diffusive-like phenomena, can arise on a network from a variety of source depending on the specifics of the network. In considering diffusion we should begin by defining a stochastic process that make physical sense for the phenomena on the network.

A continuous time random walk is a stochastic process that naturally limits to diffusion in the continuum [29, 30]. To model a reaction-diffusion process we assume that the motion of each individual particle can be expressed as a CTRW. That is to say the particles will jump from vertex to vertex on the network according to the edges present. On each vertex they will wait for a random time before randomly jumping to a connected vertex. This is analogous to spatially varying diffusion that has been previously studied in the spatial

continuum case [46].

The reactions occur between particles that occupy the same vertex. We consider the reactions to be a birth-death process of the particles. Particles will be created according to some probability, and destroyed according to a different probability. These probabilities may depend on the density of other particles on the vertex. We can then derive the equations that govern the evolution of a single particle in a time. In this manner the evolution of a single particle is subject to only the death probabilities. The birth process is included by summing the initial conditions of each single particle CTRW with the probability that a particle was created on a particular vertex at an instant in time.

The assumption that each vertex is a well mixed system is made so that the probability of a particle being destroyed in reactions is not dependent on the amount of time a particle has been waiting on the vertex. In a similar manner we also assume that each newly created particles waiting time is independent of the parent particles waiting time, similar to Model B in [38] which was first considered by Vlad and Ross [35]. The first step in this process is the derivation of the master equation for the evolution of a single particle subject to a time and space inhomogenous probability of death.

A. Single Particle CTRW Death Process Density

Consider a graph whose vertices form the set $W = \{w_1, \dots, w_J\}$ where J is the number of vertices. Let $\rho(w_j, t|w_0, 0)$ be the probability density for a random walker to be on vertex w_j at time t given it started on vertex $w_0 \in W$ at time $t = 0$.

Define $q_n(w_j, t|w_0, 0)$ as the conditional probability density for arriving at vertex w_j at time t after n steps. We define the reaction survival function, $e^{-\int_{t'}^t \beta(w_j, t'') dt''}$, as the probability that a particle stays alive from t' to t given it does not leave vertex w_j where β is a death rate that in general may depend on vertex and time. The initial condition for $n = 0$ is given by

$$q_0(w_j, t|w_0, 0) = \delta_{w_j, w_0} \delta(t - 0^+). \quad (1)$$

In general, we can write

$$q_{n+1}(w_j, t|w_0, 0) = \sum_{i=1}^J \int_0^t \Psi(w_i, w_j, t, t') e^{-\int_{t'}^t \beta(w_j, t'') dt''} q_n(w_i, t'|w_0, 0) dt' \quad (2)$$

where $\Psi(w_i, w_j, t, t')$ is the probability density of the transition to vertex w_j at time t given the random walker arrived at vertex w_i at an earlier time t' after n steps.

We assume that $\Psi(w_i, w_j, t, t')$ may be defined as a product of the independent jump probability density $\lambda(w_i, w_j)$ and $\psi(w_j, t)$.

$$\Psi(w_i, w_j, t, t') = \lambda(w_i, w_j)\psi(w_j, t - t'). \quad (3)$$

The w_j in ψ acknowledges that the waiting time density may be a function of the vertex. The conditional density for the walker to arrive at w_j at time t after any number of steps is found by summing over all n steps using Eq. (2) and Eq. (3).

$$q(w_j, t|w_0, 0) = \sum_{n=0}^{\infty} q_n(w_j, t|w_0, 0) \quad (4)$$

$$= \delta_{w_j, w_0} \delta(t - 0^+) + \sum_{n=0}^{\infty} \sum_{i=1}^J \int_0^t \Psi(w_i, w_j, t, t') e^{-\int_{t'}^t \beta(w_j, t'') dt''} q_n(w_i, t'|w_0, 0) dt' \quad (5)$$

$$= \delta_{w_j, w_0} \delta(t - 0^+) + \sum_{i=1}^J \lambda(w_i, w_j) \int_0^t \psi(w_j, t - t') e^{-\int_{t'}^t \beta(w_j, t'') dt''} q(w_i, t'|w_0, 0) dt'. \quad (6)$$

We can then define the conditional probability density for the random walker to be at vertex w_j at time t ;

$$\rho(w_j, t|w_0, 0) = \int_0^t \phi(w_j, t - t') e^{-\int_{t'}^t \beta(w_j, t'') dt''} q(w_j, t'|w_0, 0) dt', \quad (7)$$

where $\phi(w_j, t - t')$ is the probability that the particle does not jump during the period of time $t - t'$;

$$\phi(w_j, t - t') = 1 - \int_0^{t-t'} \psi(w_j, t'') dt''. \quad (8)$$

B. Single Particle CTRW Death Master Equation

The derivation of the master equations describing a CTRW death process on a network is similar to the derivations presented in [47], [48] and [38]. Formally, the integrals over probability densities should be treated as Riemann-Stieltjes integrals and care has to be

taken due to the discontinuity in the arrival density $q(w_j, t|w_0, 0)$ at time $t = 0$ [48]. To do this, write

$$q(w_j, t|w_0, 0) = \delta_{w_j, w_0} \delta(t - 0^+) + q^+(w_j, t|w_0, 0) \quad (9)$$

where q^+ is right side continuous at $t = 0$. Thus by substitution of Eq. (9) into Eq. (7) we get

$$\rho(w_j, t|w_0, 0) = \delta_{w_j, w_0} \phi(w_j, t) e^{-\int_0^t \beta(w_j, t') dt'} + \int_0^t q^+(w_j, t'|w_0, 0) e^{-\int_{t'}^t \beta(w_j, t'') dt''} \phi(w_j, t - t') dt'. \quad (10)$$

We now differentiate this equation with respect to time, using the Leibniz rule for differentiating under the integral sign, to obtain

$$\begin{aligned} \frac{\partial \rho(w_j, t|w_0, 0)}{\partial t} &= q^+(w_j, t|w_0, 0) - \int_0^t q^+(w_j, t'|w_0, 0) e^{-\int_{t'}^t \beta(w_j, t'') dt''} \psi(w_j, t - t') dt' - \\ &\quad \beta(w_j, t) \rho(w_j, t|w_0, 0) - \delta_{w_j, w_0} e^{-\int_0^t \beta(w_j, t'') dt''} \psi(w_j, t). \end{aligned} \quad (11)$$

Define the flux leaving vertex w_j at time t as

$$i(w_j, t|w_0, 0) = \delta_{w_j, w_0} e^{-\int_0^t \beta(w_j, t') dt'} \psi(w_j, t) + \int_0^t q^+(w_j, t'|w_0, 0) e^{-\int_{t'}^t \beta(w_j, t'') dt''} \psi(w_j, t - t') dt' \quad (12)$$

$$= \int_0^t q(w_j, t'|w_0, 0) e^{-\int_{t'}^t \beta(w_j, t'') dt''} \psi(w_j, t - t') dt'. \quad (13)$$

We can then rewrite Eq. (11) as

$$\frac{\partial \rho(w_j, t|w_0, 0)}{\partial t} = q^+(w_j, t|w_0, 0) - i(w_j, t|w_0, 0) - \beta(w_j, t) \rho(w_j, t|w_0, 0). \quad (14)$$

Using Eq. (6), (9) and (13), the rate of arrivals at vertex w_j can be expressed as

$$q^+(w_j, t|w_0, 0) = \sum_{i=1}^J \lambda(w_i, w_j) i(w_i, t|w_0, 0). \quad (15)$$

Now we can define ρ through an evolution law as follows

$$\frac{\partial \rho(w_j, t|w_0, 0)}{\partial t} = \sum_{i=1}^J \lambda(w_i, w_j) i(w_i, t|w_0, 0) - i(w_j, t|w_0, 0) - \beta(w_j, t) \rho(w_j, t|w_0, 0). \quad (16)$$

Following Fedotov [38] we can find an expression for the flux i in terms of ρ using Laplace transform methods on Eq. (7) and Eq. (13) respectively. We first divide both equations by $e^{-\int_0^t \beta(w_j, t'') dt''}$, this yields;

$$\mathcal{L} \left\{ \rho(w_j, t|w_0, 0) e^{\int_0^t \beta(w_j, t'') dt''} \right\} = \mathcal{L} \left\{ q(w_j, t|w_0, 0) e^{\int_0^t \beta(w_j, t') dt'} \right\} \mathcal{L} \{ \phi(w_j, t) \} \quad (17)$$

and

$$\mathcal{L} \left\{ i(w_j, t|w_0, 0) e^{\int_0^t \beta(w_j, t'') dt''} \right\} = \mathcal{L} \left\{ q(w_j, t|w_0, 0) e^{\int_0^t \beta(w_j, t') dt'} \right\} \mathcal{L} \{ \psi(w_j, t) \}. \quad (18)$$

Rearranging Eqs. (17) and (18);

$$\mathcal{L} \left\{ i(w_j, t|w_0, 0) e^{\int_0^t \beta(w_j, t') dt'} \right\} = \mathcal{L} \left\{ \rho(w_j, t|w_0, 0) e^{\int_0^t \beta(w_j, t') dt'} \right\} \frac{\mathcal{L} \{ \phi(w_j, t) \}}{\mathcal{L} \{ \psi(w_j, t) \}}. \quad (19)$$

Inverting the Laplace transform, we get;

$$i(w_j, t|w_0, 0) = \int_0^t K(w_j, t - t') \rho(w_j, t'|w_0, 0) e^{-\int_{t'}^t \beta(w_j, t'') dt''} dt' \quad (20)$$

where the memory kernel is defined by;

$$K(w_j, t) = \mathcal{L}^{-1} \left\{ \frac{\mathcal{L} \{ \psi(w_j, t) \}}{\mathcal{L} \{ \phi(w_j, t) \}} \right\}. \quad (21)$$

The master equation for the CTRW process on a network is found by the substituting Eq. (20) into Eq. (16)

$$\begin{aligned} \frac{\partial \rho(w_j, t|w_0, 0)}{\partial t} = & \sum_{i=1}^J \lambda(w_i, w_j) \int_0^t K(w_i, t - t') \rho(w_i, t'|w_0, 0) e^{-\int_{t'}^t \beta(w_i, t'') dt''} dt' - \\ & \int_0^t K(w_j, t - t') \rho(w_j, t'|w_0, 0) e^{-\int_{t'}^t \beta(w_j, t'') dt''} dt' - \beta(w_j, t) \rho(w_j, t|w_0, t_0). \end{aligned} \quad (22)$$

In the case of power law waiting time densities on a uniform grid network, this is similar to Eq. (29) in [39].

C. Ensemble CTRW Birth-Death Master Equations

To describe a birth-death process we also need to account for the creation of new particles, and hence need to consider ensembles of particles. We define $\eta(w_j, t)$ as the probability of

a particle being created at vertex w_j and at time t . Then we can define

$$u(w_j, t) = \sum_{w_0 \in W} \int_0^t \rho(w_j, t|w_0, t_0) \eta(w_0, t_0) dt_0 \quad (23)$$

as the density of a particles at vertex w_i at time t .

Taking care to differentiate Eq. (23) using Leibniz rule, we then substitute in Eq. (22) and simplify to get

$$\begin{aligned} \frac{\partial u(w_j, t)}{\partial t} &= \sum_{w_0 \in W} \left[\eta(w_0, t) \rho(w_j, t|w_0, t) + \int_0^t \eta(w_0, t_0) \frac{\partial \rho(w_j, t|w_0, t_0)}{\partial t} dt_0 \right] \quad (24) \\ &= \sum_{w_0 \in W} \int_0^t \eta(w_0, t_0) \left[\sum_{i=1}^J \int_0^t K(w_i, t-t') \lambda(w_i, w_j) e^{-\int_{t'}^t \beta(w_i, t'') dt''} \rho(w_i, t'|w_0, t_0) dt' - \right. \\ &\quad \left. \int_0^t K(w_j, t-t') \rho(w_j, t'|w_0, 0) e^{-\int_{t'}^t \beta(w_j, t'') dt''} dt' - \beta(w_j, t) \rho(w_j, t'|w_0, t_0) \right] dt_0 + \eta(w_j, t). \end{aligned} \quad (25)$$

As $\rho(w, t|w_0, t_0) = 0$ for all $t < t_0$ we can write;

$$\begin{aligned} \frac{\partial u(w_j, t)}{\partial t} &= \int_0^t \left[\sum_{i=1}^J K(w_i, t-t') \lambda(w_i, w_j) e^{-\int_{t'}^t \beta(w_i, t'') dt''} \sum_{w_0 \in W} \int_0^{t'} \rho(w_i, t'|w_0, t_0) \eta(w_0, t_0) dt_0 - \right. \\ &\quad \left. e^{-\int_{t'}^t \beta(w_j, t'') dt''} K(w_j, t-t') \sum_{w_0 \in W} \int_0^{t'} \rho(w_j, t'|w_0, t_0) \eta(w_0, t_0) dt_0 \right] dt' - \\ &\quad \beta(w_j, t) \sum_{w_0 \in W} \int_0^t \rho(w_j, t|w_0, t_0) \eta(w_0, t_0) dt_0 + \eta(w_j, t) \end{aligned} \quad (26)$$

Finally we arrive at the master equation for a CTRW with reactions on networks

$$\begin{aligned} \frac{\partial u(w_j, t)}{\partial t} &= \int_0^t \left[\sum_{i=1}^J K(w_i, t-t') \lambda(w_i, w_j) e^{-\int_{t'}^t \beta(w_i, t'') dt''} u(w_i, t') - \right. \\ &\quad \left. K(w_j, t-t') e^{-\int_{t'}^t \beta(w_j, t'') dt''} u(w_j, t') \right] dt' - \beta(w_j, t) u(w_j, t) + \eta(w_j, t). \end{aligned} \quad (27)$$

which can be written in the general form

$$\frac{\partial u(w_j, t)}{\partial t} = L[u(w_j, t)] + f(u(w_j, t)) \quad (28)$$

where

$$L[u(w_j, t)] = \int_0^t \left[\sum_{i=1}^J K(w_i, t-t') \lambda(w_i, w_j) e^{-\int_{t'}^t \beta(w_i, t'') dt''} u(w_i, t') - K(w_j, t-t') e^{-\int_{t'}^t \beta(w_j, t'') dt''} u(w_j, t') \right] dt' \quad (29)$$

is the CTRW network Laplacian and

$$f(u(w_j, t)) = -\beta(w_j, t)u(w_j, t) + \eta(w_j, t). \quad (30)$$

D. CTRW Laplacian with Exponential Waiting Times

We will now apply Eq. (27) to the case of exponential waiting times,

$$\psi(w_j, t) = \alpha(w_j) e^{-\alpha(w_j)t}. \quad (31)$$

This greatly simplifies the master equation. In general, the Laplace transform of the waiting time density, $\bar{\psi}(w_j, s) = \mathcal{L}\{\psi(w_j, t)\}$ and the Laplace transform of the survival probability $\bar{\phi}(w_j, s) = \mathcal{L}\{\phi(w_j, t)\}$ are related by $\bar{\phi}(w_j, s) = \frac{1-\bar{\psi}(w_j, s)}{s}$.

As $\psi(w_j, s)$ is exponential, then $\bar{\psi}(w_j, s) = \frac{s}{s+\alpha(w_j)}$ so $\frac{\bar{\psi}(w_j, s)}{\bar{\phi}(w_j, s)} = \alpha(w_j)$ with the inverse Laplace transform $\alpha(w_j)\delta(t)$. Thus

$$K(w_j, t) = \alpha(w_j)\delta(t). \quad (32)$$

Thus by substitution, we can rewrite the master equations Eq. (27) as

$$\frac{\partial u(w_j, t)}{\partial t} = \sum_{i=1}^J \alpha(w_i) \lambda(w_i, w_j) u(w_i, t) - \alpha(w_j) u(w_j, t) + f(u(w_j, t)) \quad (33)$$

$$= \sum_{i=1}^J L_{i,j} u(w_i, t) + f(u(w_j, t)) \quad (34)$$

where L is a member of the family of general CTRW network Laplacians defined as

$$L_{i,j} = \{\alpha(w_i) \lambda(w_i, w_j) - \alpha(w_j) \delta_{i,j}\} \quad (35)$$

In the following we consider two special cases of Eq. (35). For both cases, we assume that the jump probability and the waiting time probability are only functions of vertex degree

and time respectively. Both of these cases have been previously considered without reactions [49]. To describe the network we used the adjacency matrix

$$A_{i,j} = \begin{cases} 1 & \text{if vertices } w_i \text{ and } w_j \text{ are connected} \\ 0 & \text{otherwise.} \end{cases} \quad (36)$$

Each vertex, w_j , has a degree, k_j , that is defined as the total number of edges that link to the vertex. This is also the sum of each row of the adjacency matrix.

1. Case A

We assume that the waiting time on each vertex is identical and that the probability of jumping across an edge is equal for a given vertex. Formally, we let $\alpha(w_j) = \alpha_A$ for all $w_j \in W$ and let $\lambda(w_i, w_j) = \frac{1}{k_i}$. Thus our Laplacian becomes

$$L_{i,j} = \alpha_A \left(\frac{1}{k_i} A_{i,j} - \delta_{i,j} \right) \quad (37)$$

Note that in this case the Laplacian is not symmetric. The steady state for a CTRW with no reactions using this Laplacian, in general, will not be uniform on the vertex set.

2. Case B

An alternative is to let the waiting time on each vertex change proportionally to the vertex degree. This allows the rate of particles jumping along each edge to be constant. Formally, we let $\alpha(w_j) = \alpha_B k_j$ for all $w_j \in W$ and let $\lambda(w_i, w_j) = \frac{1}{k_i}$. Thus our Laplacian can be described as

$$L_{i,j} = \alpha_B (A_{i,j} - k_j \delta_{i,j}) \quad (38)$$

This is the well studied graph Laplacian [19] [20]. It is important to note that if a connected network is regular, i.e k_j is the same for all w_j , the cases are equivalent up to a scale factor.

III. PATTERN FORMATION

In continuum reaction-diffusion partial differential equations the concentration may vary on the spatial domain. This patterning also holds on discretisation of the spacial manifold

where the Laplacian operator is replaced by a discrete Laplace Beltrami operator [50] [51]. This can be considered as a special case of pattern formation on a discrete network. In general variation in concentrations on each vertex may occur on any network. This variation may arise in a number of different ways. Firstly if the Laplacian matrix is not symmetric in a system without reactions, there will be a build up of concentrations on vertices according to their degree. This steady state pattern will be a multiple of the eigenvector of the Laplacian with zero eigenvalue. Secondly with a non-symmetric Laplacian matrix in systems where the reactions have a finite non-zero steady state solution, the interplay between the diffusion and the reactions will cause a different pattern across the network. Unlike the no reaction case, in this pattern vertices with the same degree may have different concentrations. We refer to these two mechanisms as Laplacian pattern formation, as the patterning is driven by the non-symmetric Laplacian matrix. Lastly if the reaction terms permit a Turing instability, whereby the spatially homogeneous steady state becomes unstable in the presence of diffusion, then a Turing Pattern may form [4]. This instability is permitted for both a symmetric and non-symmetric Laplacian matrix.

A. Laplacian Pattern Formation

To completely eliminate any interplay with Turing patterns, we will consider a single species model that cannot permit a Turing instability [52].

$$\frac{\partial \mathbf{u}}{\partial t} = L \cdot \mathbf{u} + \mathbf{f}(\mathbf{u}) \quad (39)$$

where $\mathbf{u} = \left(u(w_1, t), \dots, u(w_J, t) \right)^T$ and $\mathbf{f}(\mathbf{u}) = \left(f(u(w_1, t)), \dots, f(u(w_J, t)) \right)^T$.

If we take the trivial reaction term, $\mathbf{f}(\mathbf{u}) = \mathbf{0}$, the only possible form of spatial pattern formation comes from a non-symmetric Laplacian. The master equation is then simply:

$$\frac{\partial \mathbf{u}}{\partial t} = L \cdot \mathbf{u} \quad (40)$$

It is clear that if L is non-symmetric, there will be a nonuniform rate of particle transport along the network that produces a pattern of different concentrations of particles in the long term. This concentration vector must be a multiple of the eigenvector of the Laplacian matrix with eigenvalue zero as it is a solution of the the vector \mathbf{u} that satisfies the steady state of Eq. (40), i.e.

$$L \cdot \mathbf{u} = 0. \quad (41)$$

If the reaction term $\mathbf{f}(\mathbf{u}) \neq \mathbf{0}$ and has a finite non-zero equilibrium solution then the pattern will no longer correspond to an eigenvector of the Laplacian matrix.

Define the reaction steady state \mathbf{u}^* such that the reaction term $\mathbf{f}(\mathbf{u}^*) = 0$. By considering the behaviour of $\mathbf{u} = \mathbf{u}^* + \Delta\mathbf{u}$ where $\Delta\mathbf{u}$ is some perturbation, Eq. (39) may be linearised to become

$$\frac{\partial \Delta\mathbf{u}}{\partial t} = D\mathbf{f}(\mathbf{u}^*) \cdot \Delta\mathbf{u} + L \cdot \mathbf{u}^* + L \cdot \Delta\mathbf{u}. \quad (42)$$

The steady state solutions are given by

$$\Delta\mathbf{u} = -(L + D\mathbf{f}(\mathbf{u}^*))^{-1} \cdot L \cdot \mathbf{u}^*, \quad (43)$$

provided the inverse exists where $D\mathbf{f}(\mathbf{u}^*)$ is the derivative operator of the reaction vector field \mathbf{f} at \mathbf{u}^* . This is the linear prediction of the pattern. In the case where the reaction term is linear in \mathbf{u} this equation is the exact solution for the pattern. It should also be noted that in the case of a symmetric Laplacian $L \cdot \mathbf{u}^* = \mathbf{0}$, as the constant vector is always a null vector of a symmetric Laplacian. This equation does not hold without reactions as a non-symmetric Laplacian is in general non-invertible.

This type of pattern formation is very different from a Turing pattern. A Turing pattern is formed by an instability in the dynamics whereby an otherwise stable solution is made unstable by the presence of diffusion. It is a bifurcation phenomena as the diffusion must reach a critical value before the solution becomes unstable. In this case however we have a pattern that will form for any amount of diffusion, the stability of the solution does not change but rather the solution itself is a function of the diffusion. To examine this we introduce a scale parameter s for our Laplacian whereby the linear predictor for the pattern becomes

$$\Delta\mathbf{u} = -(sL + D\mathbf{f}(\mathbf{u}^*))^{-1} sL \cdot \mathbf{u}^* \quad (44)$$

The new scalar parameter that governs the speed of diffusion in the system. In the limit $s \rightarrow 0$ we have;

$$\Delta\mathbf{u} = \mathbf{0} \quad (45)$$

which corresponds to no pattern, and each vertex taking the equilibrium values of the reactions. In the limit $s \rightarrow \infty$ care has to be taken with the existence of the inverse. Taking Eq. (44) and multiplying through by $(sL + D\mathbf{f}(\mathbf{u}^*))$ dividing by s and taking the limit we

have

$$\lim_{s \rightarrow \infty} \left(L + \frac{D\mathbf{f}(\mathbf{u}^*)}{s} \right) \Delta \mathbf{u} = -L \cdot \mathbf{u}^* \quad (46)$$

$$L \cdot \Delta \mathbf{u} + L \cdot \mathbf{u}^* = 0 \quad (47)$$

$$L \cdot \mathbf{u} = 0 \quad (48)$$

and so the pattern will be equivalent to the case with no reactions. In this way it can be seen that this type of pattern formation is the mixing of the pattern formation from the non-symmetric Laplacian and the reaction equilibrium.

B. Turing Pattern Formation

Turing pattern formation can arise from a Turing instability [4]. Such instabilities were originally proposed by Turing as a possible explanation for morphogenesis. We consider a general two species reaction-diffusion system with particle concentrations u and v . The master equations, [see Eq. (34)], can be written as

$$\frac{\partial u(w_j, t)}{\partial t} = \sum_{i=1}^J \alpha_u L_{i,j} u(w_i, t) + f(u(w_j, t), v(w_j, t)) \quad (49)$$

and

$$\frac{\partial v(w_j, t)}{\partial t} = \sum_{i=1}^J \alpha_v L_{i,j} v(w_i, t) + g(u(w_j, t), v(w_j, t)) \quad (50)$$

where the functions $f(u(w_j, t), v(w_j, t))$ and $g(u(w_j, t), v(w_j, t))$ incorporate the creation and destruction probabilities. ie;

$$f(u(w_j, t), v(w_j, t)) = \eta_u(w_j, t) - \beta_u(w_j, t)u(w_j, t) \quad (51)$$

$$= \eta_u(u(w_j, t), v(w_j, t)) - \beta_u(u(w_j, t), v(w_j, t))u(w_j, t) \quad (52)$$

and similarly for $g(u(w_j, t), v(w_j, t))$. Here note that the α_u and α_v is factored out of the Laplacian, $L_{i,j}$ so that the operator is the same in both equations.

1. Linear Stability Analysis

To consider Turing instabilities, we first rewrite Eqs. (49) and (50) in vector form

$$\frac{\partial \mathbf{X}}{\partial t} = \Lambda \mathbf{X} + F(\mathbf{X}) \quad (53)$$

where

$$\begin{aligned}
\mathbf{X} &= \left(u(w_1, t), \dots, u(w_J, t), v(w_1, t), \dots, v(w_J, t) \right)^T \\
&= \left(X_1, \dots, X_J, X_{J+1}, \dots, X_{2J} \right)^T, \\
F(\mathbf{X}) &= \left(f(X_1, X_{J+1}), \dots, f(X_J, X_{2J}), g(X_1, X_{J+1}), \dots, g(X_J, X_{2J}) \right)^T \\
&= \left(F_1, \dots, F_J, F_{J+1}, \dots, F_{2J} \right)^T \\
\text{and } \Lambda &= \begin{pmatrix} \alpha_u L & 0 \\ 0 & \alpha_v L \end{pmatrix}.
\end{aligned}$$

Linearising about the steady state \mathbf{X}^* with $F(\mathbf{X}^*) = 0$ and $\mathbf{X} = \mathbf{X}^* + \Delta\mathbf{X}$. We then substitute this into Eq. (53) to get

$$\frac{\partial \Delta\mathbf{X}}{\partial t} = (\Lambda + DF(\mathbf{X}^*)) \cdot \Delta\mathbf{X} + \Lambda \cdot \mathbf{X} \quad (54)$$

where

$$DF(\mathbf{X}^*)_{i,j} = \left. \frac{\partial F_i}{\partial X_j} \right|_{\mathbf{X}^*}. \quad (55)$$

We now apply the affine transform $\Delta\mathbf{Y} = \Delta\mathbf{X} + (\Lambda + DF(\mathbf{X}^*))^{-1} \cdot \Lambda \cdot \mathbf{X}^*$ to Eq. (54) yielding

$$\frac{\partial \Delta\mathbf{Y}}{\partial t} = (\Lambda + DF(\mathbf{X}^*)) \cdot \Delta\mathbf{Y} \quad (56)$$

which gives solutions of the form

$$\Delta\mathbf{Y} = \sum_{j=1}^J e^{\mu_j t} P_j(t) \nu_j \quad (57)$$

where μ_j is the j^{th} eigenvalue of $(\Lambda + DF(\mathbf{X}^*))$ with corresponding eigenvector ν_j . P_j is a polynomial in t for repeated eigenvalues. The long time behaviour of $\Delta\mathbf{Y}$ is then approximated by

$$\Delta\mathbf{Y} \sim e^{\mu^* t} P^*(t) \nu^* \quad (58)$$

where μ^* corresponds to the real component of the largest eigenvalue.

In the linear stability analysis the concentrations of the two species evolve as

$$\mathbf{X} \sim e^{\mu^* t} P(t) \nu^* + \mathbf{X}^* - (\Lambda + DF(\mathbf{X}^*))^{-1} \cdot \Lambda \cdot \mathbf{X}^* \quad (59)$$

2. Dispersion Relation

In the continuum case the real components of the eigenvalues (i.e.: stability) of the homogeneous steady state can be plotted against spatial frequency to obtain a dispersion relation showing the range of spatial frequencies that will grow with time. In an analogous manner for the network case, we plot the stability of the reaction-diffusion system as a function of a scale parameter s equivalent to scaling the waiting time for both species on the network:

$$\frac{\partial \mathbf{X}}{\partial t} = s\Lambda.\mathbf{X} + F(\mathbf{X}) \quad (60)$$

When s is zero there is no coupling between vertices and each vertex will be in equilibrium according to the reaction equations. We identify two critical values of s greater than zero from our linear stability analysis. Firstly the Laplacian type pattern arising from the coupling of reactions to diffusion may change to a Turing pattern at a critical value of s . As s is further increased the Turing pattern, if it occurs, will persist till the second critical value when the pattern reverts back to a Laplacian type pattern.

IV. EXAMPLES OF PATTERN FORMATION

To illustrate the properties of both the Laplacian and Turing patterns on networks the master equations with exponential waiting times were solved numerically. For the Laplacian patterns, Eq. (34) was solved with Logistic reaction kinetics using the Case A Laplacian operator. The Turing patterns were examined by solving Eqs. (49) and (50) with Gierer-Meinhardt reaction kinetics and both the Case A and Case B Laplacian operators. In both cases the equations were solved on random networks generated by the Barabási-Albert algorithm [3], and the Watts-Strogatz algorithm [53]. The equations were also solved on deterministic binary tree networks.

The first reaction kinetics that we consider is the logistic equation [54],

$$f(u(x, t)) = ru(x, t)(1 - u(x, t)) \quad (61)$$

where r is a constant. This governs the growth rate of a single species. In the following examples we will take $r = 1$. When applied to a network, this simple example could be considered a model for animal populations in a set of connected habitats, where the

population is constrained by natural limits. The reaction-diffusion master equation in this case is found by substituting Eq. (61) into Eq. (39).

$$\frac{\partial u(w_j, t)}{\partial t} = \sum_{i=1}^J L_{i,j} u(w_i, t) + u(w_i, t)(1 - u(w_i, t)) \quad (62)$$

Here L is the Case A Laplacian with $\alpha = 1$, i.e. $L_{i,j} = \frac{A_{i,j}}{k_i} - \delta_{i,j}$.

The second model we consider has Gierer-Meinhardt reaction kinetics [5]. This is a two species model that permits Turing instabilities. The reaction terms in the model are:

$$f(u(x, t), v(x, t)) = c\rho \frac{u(x, t)^2}{v(x, t)} - \mu u(x, t) + \rho_0\rho \quad (63)$$

and

$$g(u(x, t), v(x, t)) = c_d\rho u(x, t)^2 - \nu v(x, t) \quad (64)$$

We can apply this model to a network setting by substituting Eqs. (63) and (64) in Eqs. (49) and (50):

$$\frac{\partial u(w_j, t)}{\partial t} = c\rho \frac{u(w_j, t)^2}{v(w_j, t)} - \mu u(w_j, t) + \rho_0\rho + \alpha_u \sum_{i=1}^J L_{i,j} u(w_i, t) \quad (65)$$

$$\frac{\partial v(w_j, t)}{\partial t} = c_d\rho u(w_j, t)^2 - \nu v(w_j, t) + \alpha_v \sum_{i=1}^J L_{i,j} v(w_i, t). \quad (66)$$

In the following we use;

$$\rho_0 = 1, \quad \rho = 1, \quad \nu = \frac{7}{32}, \quad \mu = \frac{5}{256}, \quad c = 1, \text{ and } c_d = \frac{5}{128}. \quad (67)$$

For the Case A Laplacian we will use:

$$\alpha_u = 1 \text{ and } \alpha_v = \frac{1}{256}. \quad (68)$$

To place the Case B Laplacian, i.e. $L_{i,j} = A_{i,j} - k_i\delta_{i,j}$, on a comparable footing to the Case A we rescale the parameters α_u and α_v to ensure that the mean waiting time across the network is comparable in both cases. Explicitly

$$\alpha_u = \frac{J}{\sum_{j=1}^J k_j} \text{ and } \alpha_v = \left(\frac{1}{256}\right) \frac{J}{\sum_{j=1}^J k_j}. \quad (69)$$

A. Barabási-Albert Network

The Barabási-Albert (BA) network is a random network with a power law distribution of vertex degrees [3]. The network is iteratively generated by adding a vertex at each step that connects to k existing vertices where the probability of attachment is proportional to the degree of the existing vertices.

We first consider a purely diffusive process governed by the Case A Laplacian on BA networks. In this case, the concentration on each vertex is proportional to its degree, resulting in the shape of the concentrations to be similar to a power law shape as shown in Fig. 1. This distribution, which corresponds to the eigenvector of the Laplacian with a zero eigenvalue, is monotonic with increasing vertex degree.

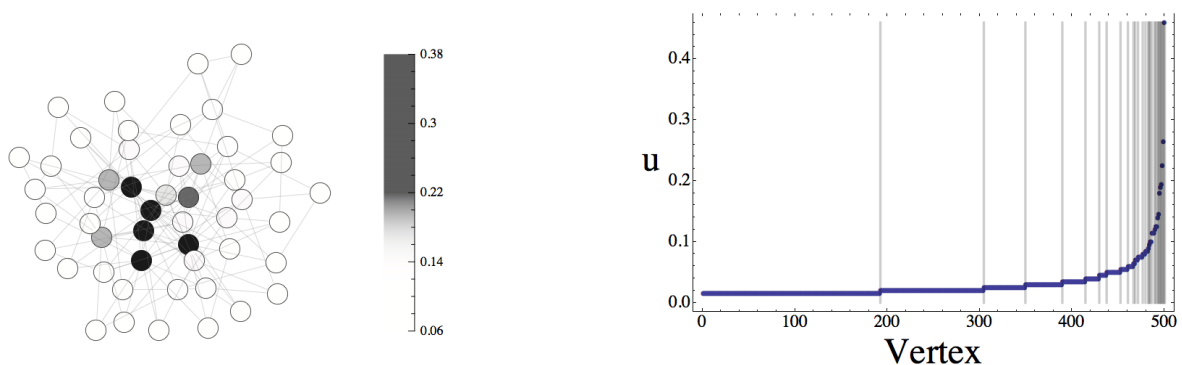


FIG. 1. (Colour Online) Case A Laplacian diffusion on a BA network with $k = 3$. A characteristic pattern of a network with 50 vertices (*left*) and the distribution of concentrations on a 500 vertex network (*right*). The vertical lines demark regions of different vertex degree

With the addition of the logistic reaction term, concentrations across the network change. The overall power law shape is still present, however the pattern is no longer monotonic with respect to vertex degree. The linear predictor of the pattern across the network, Eq. (43), is a good approximation near the reaction steady state, see Fig. 2. The mean of the concentration across the network is reduced from the reaction equilibrium value.

When the reactions are governed by the Gierer-Meinhardt model, Turing instabilities can arise producing patterns different to the Laplacian patterns. We first consider the patterns when the Case A Laplacian is used, a representative example is shown in Fig. 3. The exact pattern is determined by the initial conditions of the system. This multi-stability is in

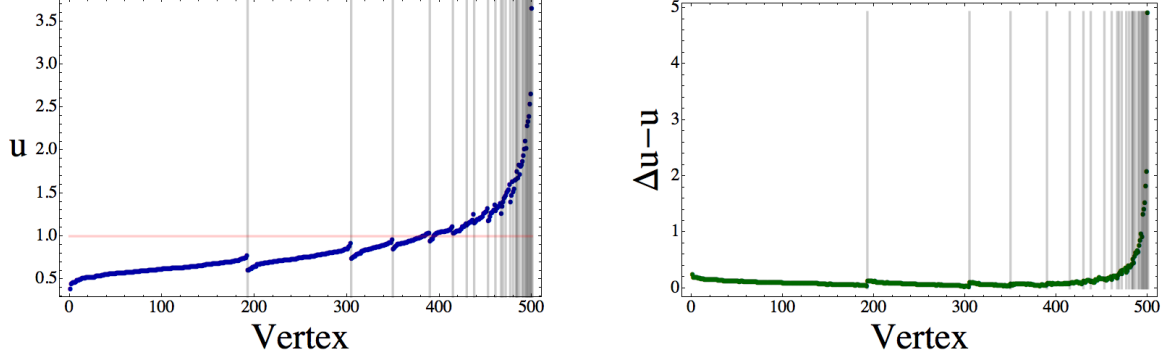


FIG. 2. (Colour Online) Case A Laplacian with logistic reaction kinetics on a BA network with $k = 3$. Concentration (*left*) and difference of linear predictor and concentration (*right*). The pale horizontal line is the reaction steady state value and that the data is ordered according to concentration within each segment of constant vertex degree. The vertical lines demark regions of different vertex degree

contrast to the Laplacian patterns that have no initial condition dependence. In all observed Turing patterns the concentrations for both types of particles are split on vertices with low degree. There is also an increasing concentration as a function of vertex degree as seen in the previous BA patterns, especially for the concentration of u particles.

When considering the Case B Laplacian, as shown in Fig. 4, the patterns shown are clearly very different to those in Fig. 3. There is a splitting of concentration across all vertex degree segments and the lower level shows practically no increase in concentration as a function of vertex degree. Moreover the concentrations achieved are higher and lower for u and v respectively when compared to Case A. Unlike for the Case A model, the patterns exhibited by u and v have similar profiles.

It is interesting to note the change in mean concentration for the two Turing patterns. For the Case A pattern we have both the the mean of u and v greater then the reaction steady state value with no diffusion. For Case B, the opposite is true and the mean values are less then the reaction steady state values.

The dispersion relations for Case A and B are plotted in Fig. 5. The Turing instability occurs over a larger range in Case B than Case A.

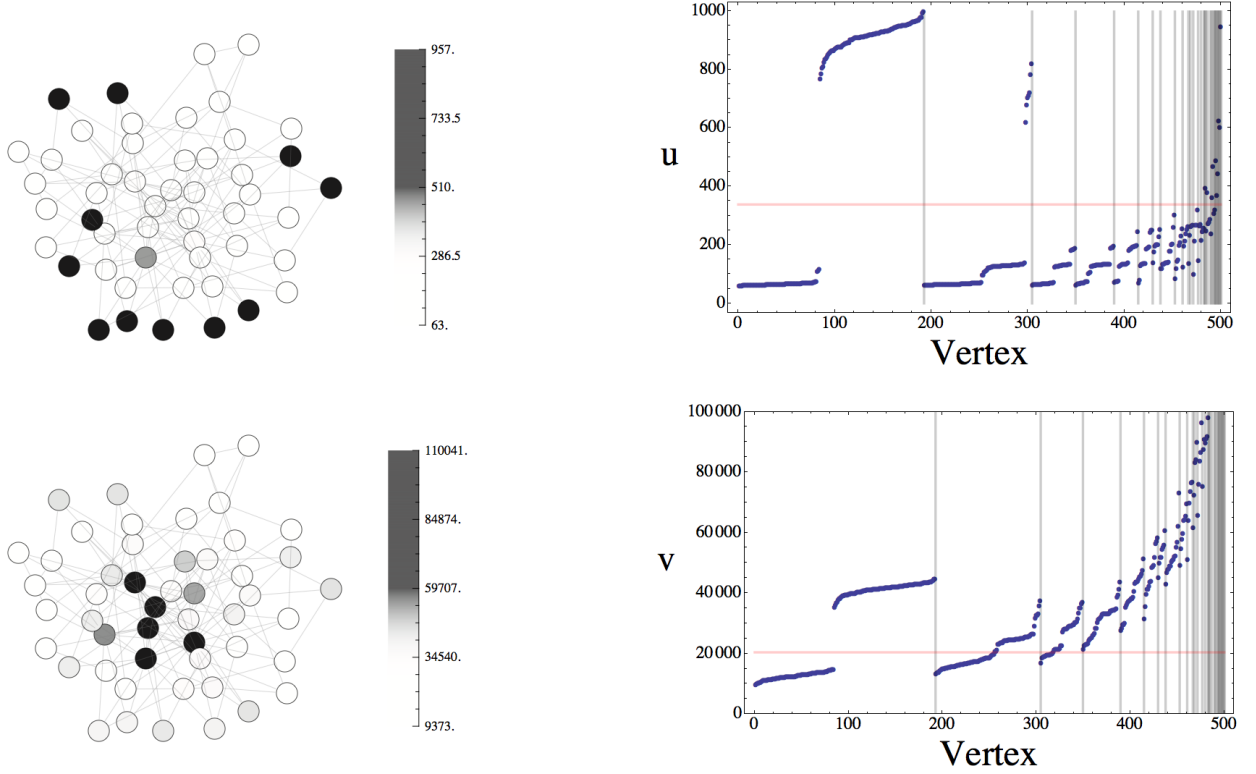


FIG. 3. (Colour Online) Case A Laplacian Gierer-Meinhardt reaction diffusion on a BA network with $k = 3$. Concentration of u (top) and v (bottom) on 50 (left) and 500 (right) vertex networks. The horizontal line gives the reaction steady state.

B. Watts-Strogatz Network

The Watts-Strogatz (WS) network is a random network characterised by the small world property of having a low graph diameter [53]. The network is generated by creating a ring lattice where each vertex is connected to k adjacent vertices. Then each subsequent edge may be reconnected with some probability p to some other vertex chosen uniformly from all vertices.

Once again we first consider a purely diffusive process governed by the Case A Laplacian. The concentration on each vertex is proportional to the degree of the vertex as shown in Fig. 6.

The same network with logistic reaction kinetics is shown in Fig. 7. Similarly to the BA network, each segment of vertices with identical degree shows a gentle slope in concentration with tapered boundaries. However the underlying concentration distribution is similar to

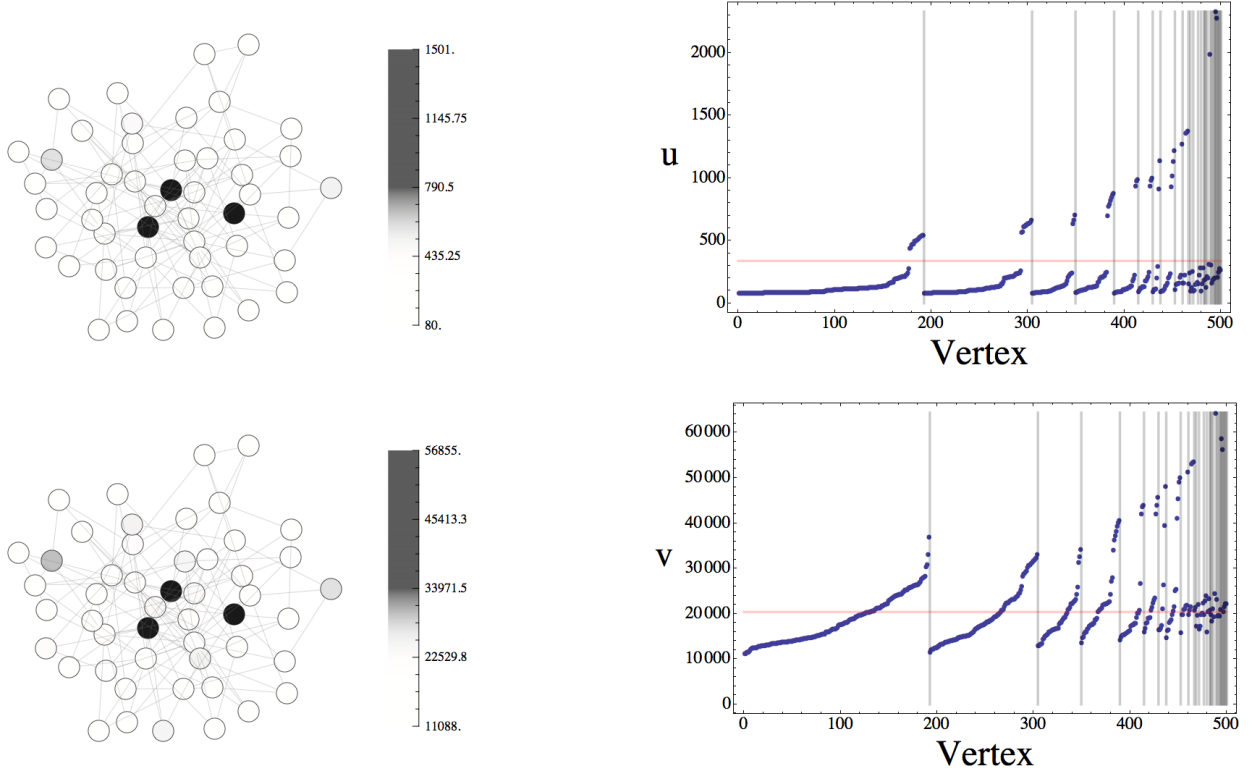


FIG. 4. (Colour Online) Case B Laplacian Gierer-Meinhardt reaction diffusion on a BA network with $k = 3$. Concentration of u (top) and v (bottom) on 50 (left) and 500 (right) vertex networks. The horizontal line gives the reaction steady state

that of the previous case. We see that the linear predictor is a good approximation when the concentration is near the reaction steady state value.

We consider the Gierer-Meinhardt reaction kinetics with both Case A and Case B Laplacian operators as shown in Figs. 8 and 9 respectively. In both cases, the distribution of concentrations is bimodal for each vertex degree.

The example using the Case B Laplacian exhibits very similar patterns to those using the Case A. Similarly to the BA network, the highest concentrations in the second example are always increasing in contrast to the the first example. Unlike the patterns on the BA network, the concentrations for both cases are at comparable quantities.

Dispersion relations for the Case A and Case B models are shown in Fig. 10. Unlike in the BA network, both Laplacian operators permit dispersion relations with almost indistinguishable profiles.

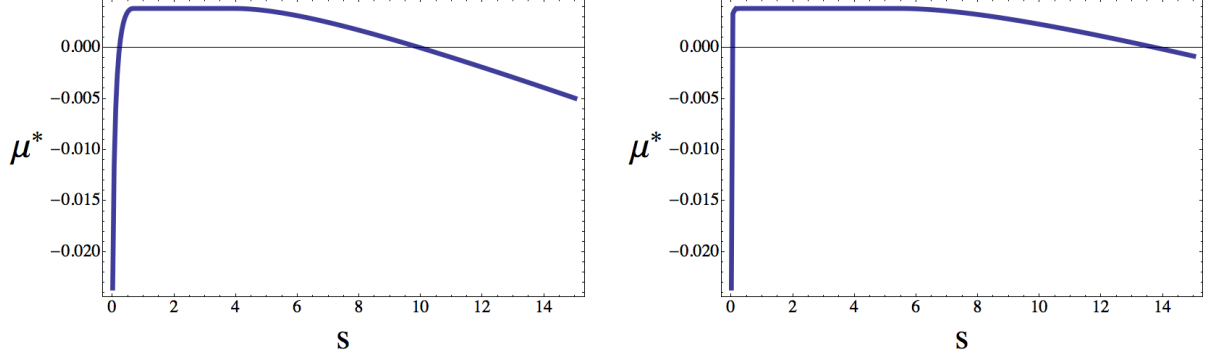


FIG. 5. (Colour Online) Dispersion Relation for Case A (*left*) and Case B (*right*) Laplacian Gierer-Meinhardt reaction diffusion on a BA network with $k = 3$.

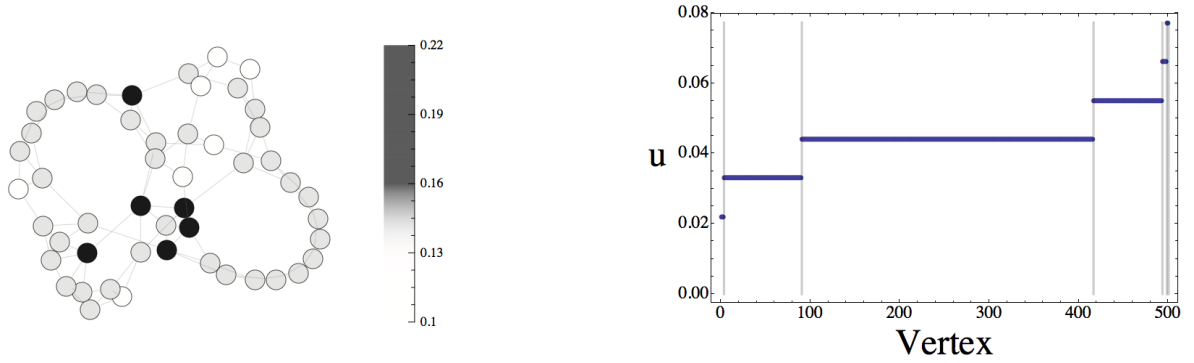


FIG. 6. (Colour Online) Case A Laplacian diffusion on a WS network with $k = 3$ and $p = 0.1$. A characteristic pattern of a network with 50 vertices (*left*) and the distribution of concentrations on a 500 vertex network (*right*). The vertical lines demark regions of different vertex degree.

C. Binary Tree Network

A binary tree is a deterministic network whereby starting with a single vertex, we connect two new vertices which are in turn each connected to another two new vertices and this process is repeated until the desired number of vertices is reached.

The concentrations for a system with no reactions and a Case A Laplacian are shown in Fig. 11.

There are three distinct concentrations across the network as the concentrations are proportional to vertex degree.

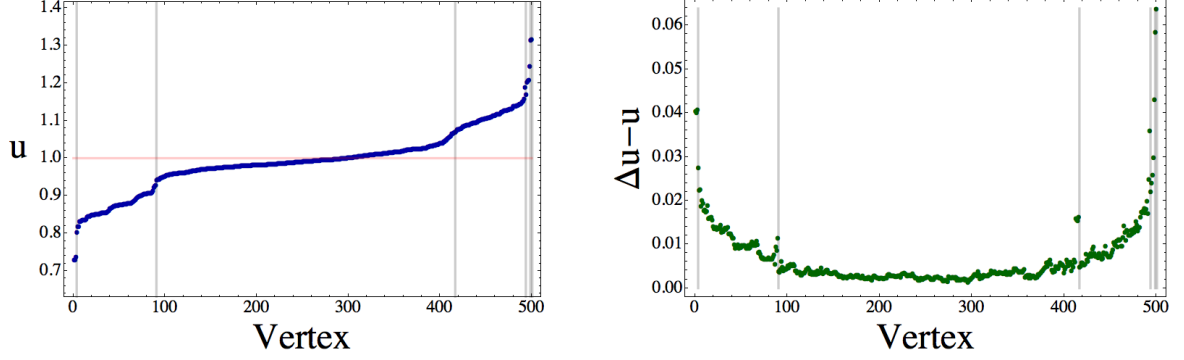


FIG. 7. (Colour Online) Case A Laplacian with logistic reaction kinetics on a WS network with $k = 3$ and $p = 0.1$. Concentration (left) and difference of linear predictor and concentration (right). The pale horizontal line is the reaction steady state value and that the data is ordered according to concentration within each segment of constant vertex degree. The vertical lines demark regions of different vertex degree.

With the addition of the logistic reaction kinetics, concentrations are no longer simply proportional to vertex degree as shown in Fig. 12.

Steady state concentrations for Gierer-Meinhardt reaction kinetics and both Case A and Case B Laplacian operators are shown in Figs. 13 and 14 respectively.

The dispersion relation of the Case A and B models as shown in Fig. 15 differ significantly to those on the BA and WS networks [see Figs. 5 and 10].

V. SUMMARY AND DISCUSSION

In this paper we have derived the generalized master equation for reaction diffusion processes on networks based on the CTRW as the underlying stochastic process. We assumed that the vertices of the network can be occupied by many particles with the reactions occurring amongst the particles on the same vertex. The reactions were assumed to be governed by the same reaction kinetics on each vertex. The CTRW models particles jumping between vertices and reaction kinetics were incorporated into this as birth and death processes. We used the CTRW framework to derive a family of Laplacian operators that govern the diffusion on the network. These operators are dependent on the waiting time probability density at each vertex and the jumping probability density between vertices. In the case

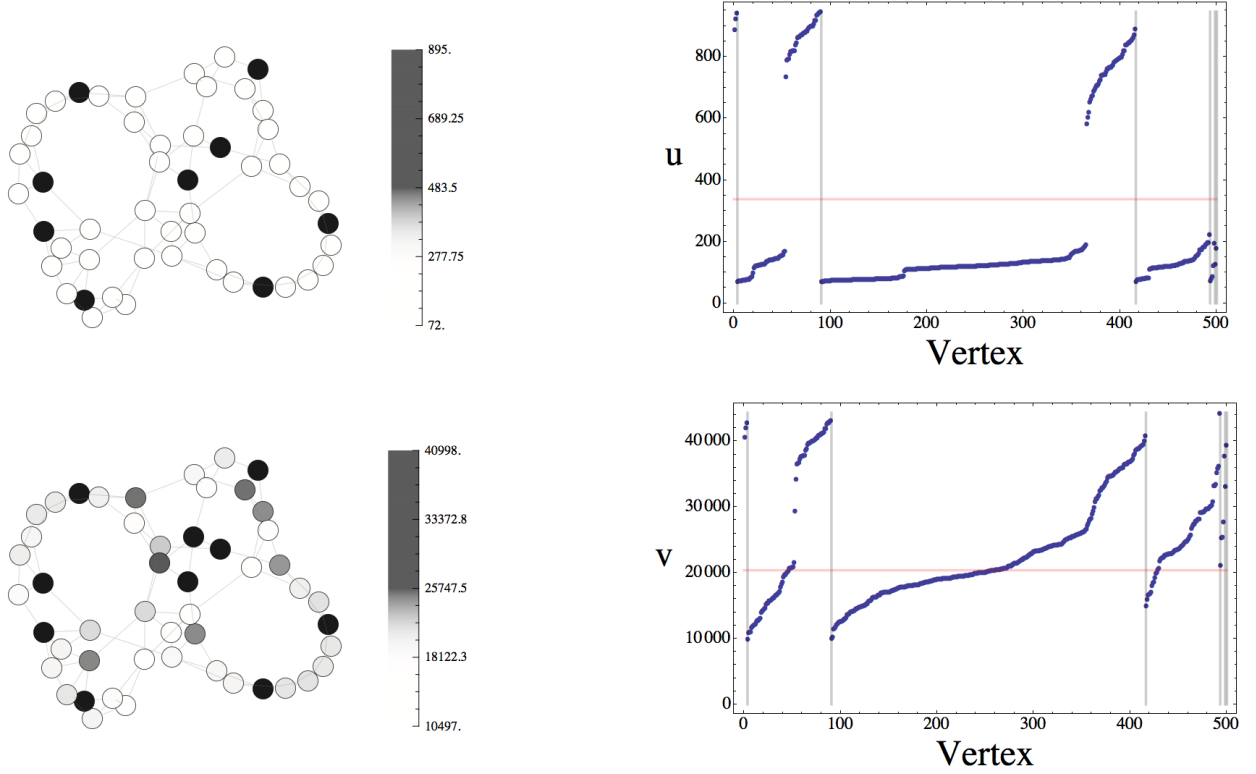


FIG. 8. (Colour Online) Case A Laplacian Gierer-Meinhardt reaction diffusion on a WS network with $k = 3$ and $p = 0.1$. Concentration of u (top) and v (bottom) on 50 (left) and 500 (right) vertex networks. The horizontal line gives the reaction steady state.

of non-exponential waiting time densities these operators convolve the reaction and transport processes. However in the case of exponential waiting times the operators are purely transport operators.

In general it is to be expected that the CTRW network reaction-diffusion model can lead to unequal concentrations of particles across the vertices. We investigated this pattern formation in the concentrations of particles. We considered the jumping probability to be equal across any edge from a given vertex and we considered the waiting time densities to be exponential, for two choices of the rate parameter; Case A where the rate parameter was taken to be proportional to the vertex degree and Case B where the rate parameter was taken to be the same for all edges.

We identified three distinct pattern formation mechanisms in our CTRW network reaction-diffusion models. In the case of symmetric network Laplacian operators pattern

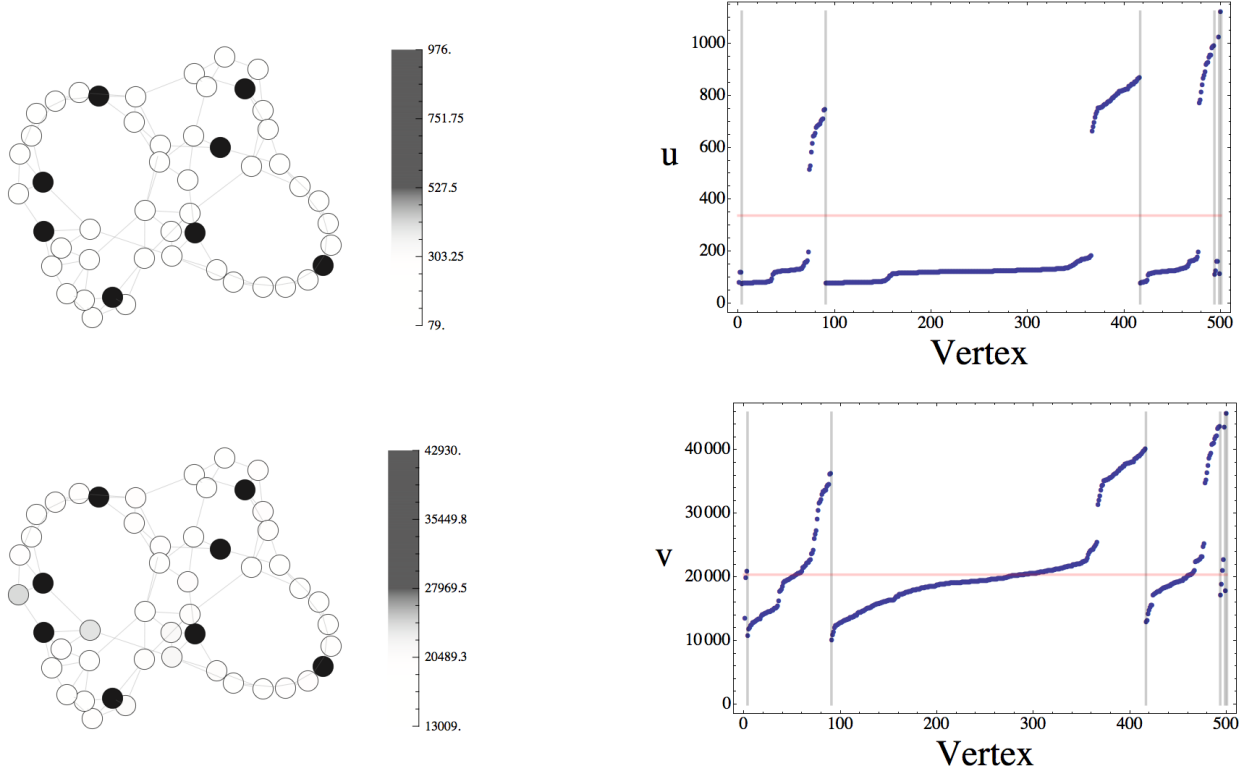


FIG. 9. (Colour Online) Case B Laplacian Gierer-Meinhardt reaction diffusion on a WS network with $k = 3$ and $p = 0.1$. Concentration of u (top) and v (bottom) on 50 (left) and 500 (right) vertex networks. The horizontal line gives the reaction steady state.

formation followed a Turing mechanism whereby the steady state of the reaction dynamics, homogeneous across the vertices, became de-stabilized by the jumps resulting in a non-homogeneous pattern across the vertices. The Turing mechanism can also result in pattern formation when the network Laplacian is non-symmetric but other pattern formation mechanisms can occur in this case too. Secondly the use of the non-symmetric Laplacian may by itself, lead to a build up in concentrations on vertices according to their degree. Thirdly if the non-symmetric Laplacian is coupled with reactions that have a finite non-zero steady state then the interplay between the two can result in a different pattern across the network. The different signatures of these patterns may prove useful in elucidating the underlying transport processes in networks when this is not known at the outset.

The family of Laplacians we have derived should be used when the underlying process may be represented by a CTRW. This embodies a large class of diffusive processes on networks.

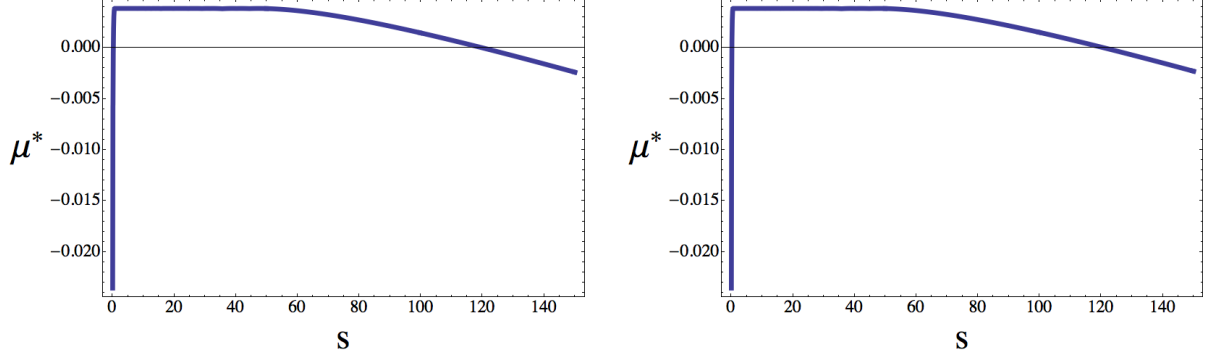


FIG. 10. (Colour Online) Dispersion Relation for Case A (*left*) and Case B (*right*) Laplacian Gierer-Meinhardt reaction diffusion on a 500 vertex WS network with $k = 3$ and $p = 0.1$.

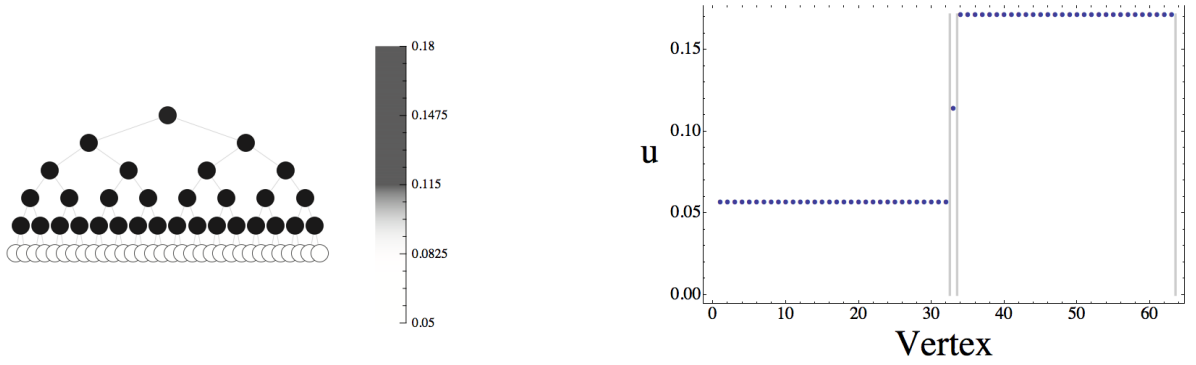


FIG. 11. (Colour Online) Case A Laplacian diffusion on a 63 vertex binary tree network. The vertical lines demark sets of vertices with different degrees.

By considering the underlying stochastic process, the ad-hoc choices of transport operators are constrained resulting in a physically consistent model of diffusion on networks. Our models of reaction-diffusion on networks are capable of reproducing a wide range of observed dynamics, as exemplified by our pattern formation examples.

-
- [1] A. L. Barabási and Z. N. Oltvai, Nat. Rev. Genet. **5**, 101 (2004).
 - [2] R. Zallen, *The physics of amorphous solids*, Vol. 26 (Wiley Online Library, 1983).
 - [3] A.-L. Barabási and R. Albert, Science **286**, 509 (1999).

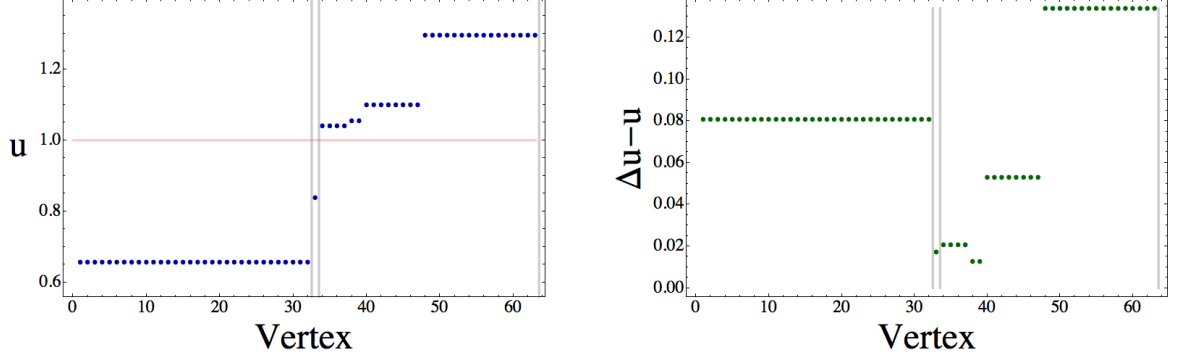


FIG. 12. (Colour Online) Case A Laplacian logistic reaction diffusion on a 63 vertex binary tree network. Concentration (left) and difference of linear predictor and concentration (right). The pale horizontal line is the reaction steady state value and that the data is ordered according to concentration within each segment of constant vertex degree.

- [4] A. M. Turing, Phil. Trans. R. Soc. B **237**, 37 (1952).
- [5] A. Gierer and H. Meinhardt, Biol. Cybern. **12**, 30 (1972).
- [6] S. Kondo and T. Miura, Science **329**, 1616 (2010).
- [7] A. Madzvamuse, E. A. Gaffney, and P. K. Maini, J. Math. Biol. **61**, 133 (2010).
- [8] H. Meinhardt, Interface Focus **2**, 407 (2012).
- [9] P. K. Maini, T. E. Woolley, R. E. Baker, E. A. Gaffney, and S. S. Lee, Interface Focus **2**, 487 (2012).
- [10] Q. Ouyang and H. L. Swinney, Nature **352**, 610 (1991).
- [11] G. Sun, Z. Jin, Q. X. Liu, and L. Li, J. Stat. Mech. Theor. Exp. **2007**, P11011 (2007).
- [12] O. Stancevic, C. Angstmann, J. M. Murray, and B. I. Henry, (2012), arXiv:1209.2772 [q-bio].
- [13] M. Mimura and J. D. Murray, J. Theor. Biol. **75**, 249 (1978).
- [14] H. G. Othmer and L. E. Scriven, J. Theor. Biol. **32**, 507 (1971).
- [15] V. Colizza, R. Pastor-Satorras, and A. Vespignani, Nat. Phys. **3**, 276 (2007).
- [16] L. K. Gallos and P. Argyrakis, Phys. Rev. Lett. **92**, 138301 (2004).
- [17] W. Horsthemke, K. Lam, and P. K. Moore, Phys. Lett. A **328**, 444 (2004).
- [18] L. Diambra and L. da Fontoura Costa, Phys. Rev. E **73**, 031917 (2006).
- [19] H. Nakao and A. S. Mikhailov, Nature Physics **6**, 544 (2010).
- [20] S. Hata, H. Nakao, and A. S. Mikhailov, EPL. **98**, 64004 (2012).

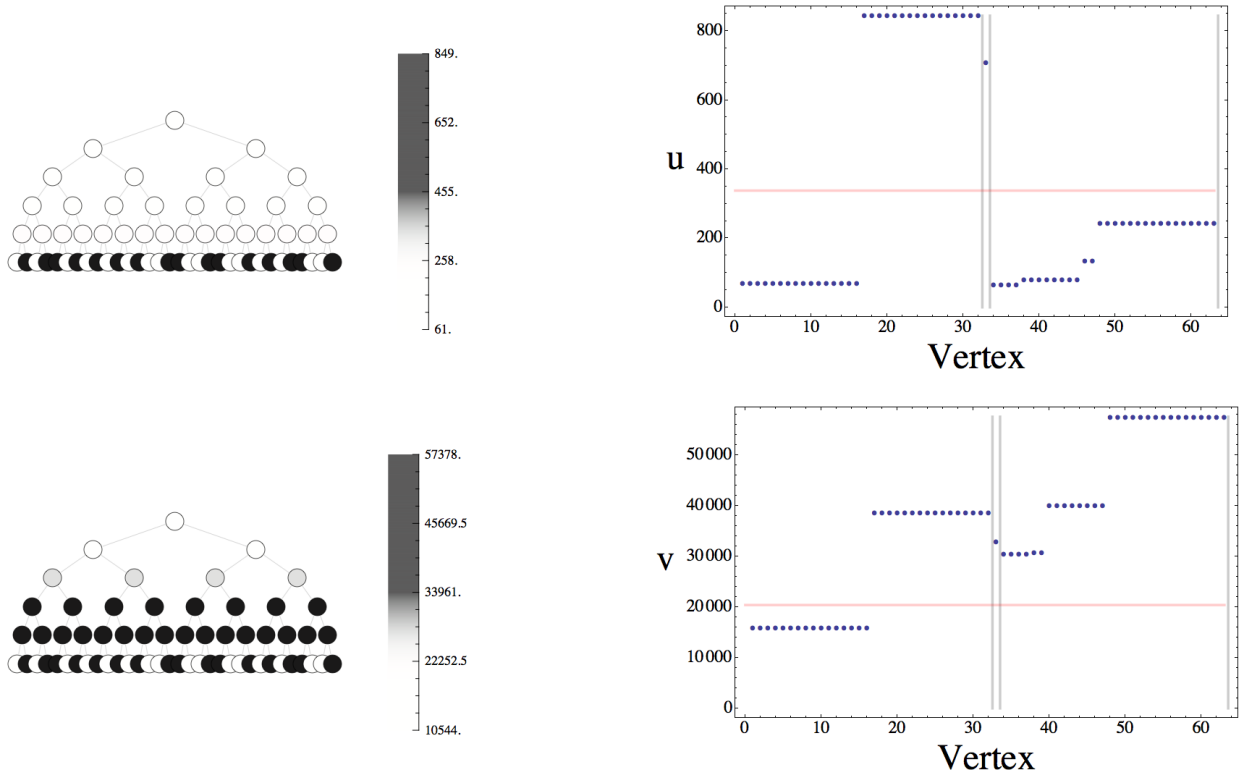


FIG. 13. (Colour Online) Case A Laplacian Gierer-Meinhardt reaction diffusion on a 63 vertex binary tree network. Concentration of u (*top*) and v (*bottom*). The horizontal line gives the reaction steady state.

- [21] M. Wolfrum, *Physica D* **241**, 1351 (2012).
- [22] N. E. Kouvaris, H. Kori, and A. S. Mikhailov, (2012), arXiv:1206.4447 [nlin].
- [23] L. Bachelier, *Théorie de la spéculation* (Gauthier-Villars, 1900).
- [24] K. Pearson, *Nature* **72**, 342 (1905).
- [25] A. Einstein, *Annalen der Physik* **322**, 549 (1905).
- [26] S. Havlin and D. Ben-Avraham, *Advances in Physics* **36**, 695 (1987).
- [27] J. D. Noh and H. Rieger, *Phys. Rev. Lett.* **92**, 118701 (2004).
- [28] S. Condamin, O. Bénichou, V. Tejedor, R. Voituriez, and J. Klafter, *Nature* **450**, 77 (2007).
- [29] E. Montroll and G. Weiss, *J. Math. Phys.* **6**, 167 (1965).
- [30] H. Scher and M. Lax, *Phys. Rev. B* **7**, 4491 (1973).
- [31] J. Klafter and I. M. Sokolov, *First Steps in Random Walks: From Tools to Applications* (Oxford University Press, USA, 2011).

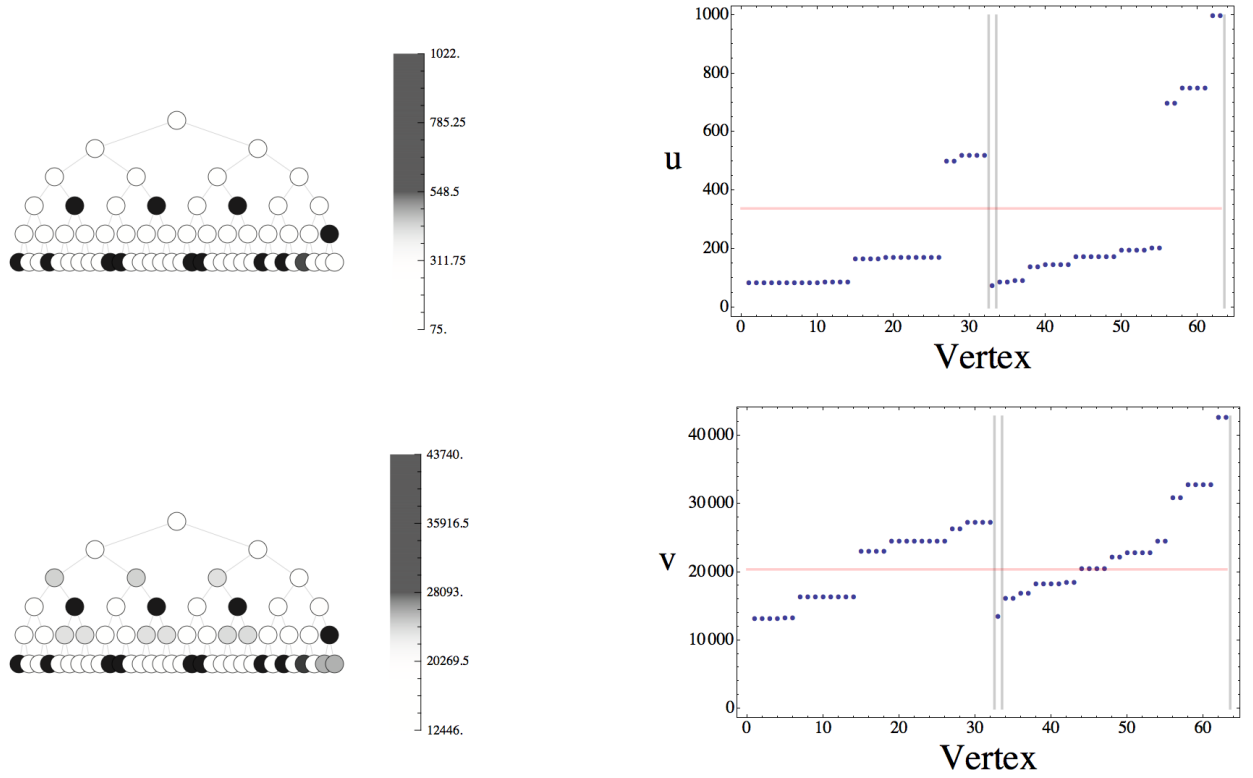


FIG. 14. (Colour Online) Case B Laplacian Gierer-Meinhardt reaction diffusion on a 63 vertex binary tree network. Concentration of u (*top*) and v (*bottom*). The horizontal line gives the reaction steady state.

- [32] I. M. Sokolov, M. G. W. Schmidt, and F. Sagués, Phys. Rev. E **73**, 031102 (2006).
- [33] B. I. Henry, T. A. M. Langlands, and S. L. Wearne, Phys. Rev. E **74**, 031116 (2006).
- [34] T. A. M. Langlands, B. I. Henry, and S. L. Wearne, Phys. Rev. E **77**, 021111 (2008).
- [35] M. O. Vlad and J. Ross, Phys. Rev. E **66**, 061908 (2002).
- [36] S. Eule, R. Friedrich, F. Jenko, and I. M. Sokolov, Phys. Rev. E **78**, 060102 (2008).
- [37] V. Méndez, S. Fedotov, and W. Horsthemke, *Reaction-Transport Systems: mesoscopic foundations, fronts, and spatial instabilities* (Springer, 2010).
- [38] S. Fedotov, Phys. Rev. E **81**, 011117 (2010).
- [39] E. Abad, S. B. Yuste, and K. Lindenberg, Phys. Rev. E **81**, 031115 (2010).
- [40] I. Simonsen, Physica A **357**, 317 (2005).
- [41] D. Le Bihan, J. F. Mangin, C. Poupon, C. Clark, S. Pappata, N. Molko, and H. Chabriat, J. Magn. Reson. Im. **13**, 534 (2001).

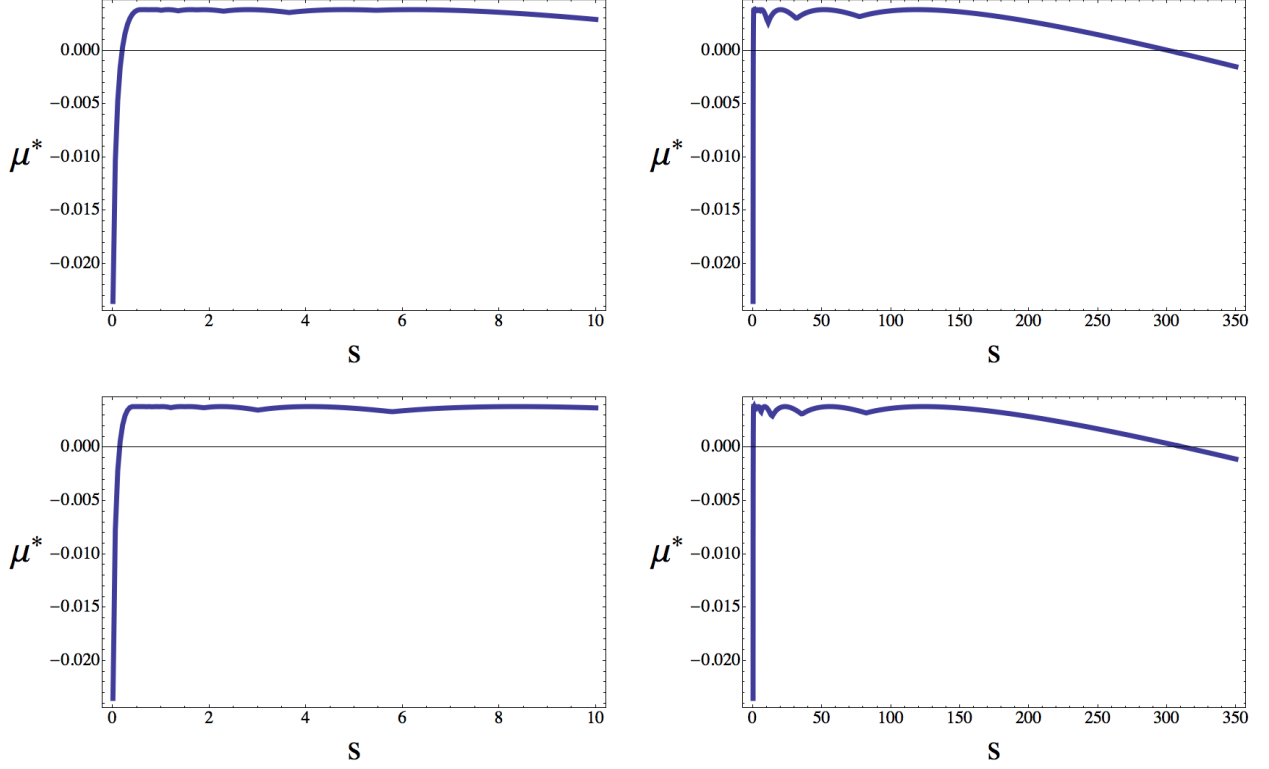


FIG. 15. (Colour Online) Full (right) and magnified (left) dispersion relations of Case A (top) and Case B (bottom) Laplacians on a 63 vertex binary tree network with Gierer-Meinhardt reaction kinetics.

- [42] A. Raj, A. Kuceyeski, and M. Weiner, *Neuron* **73**, 1204 (2012).
- [43] V. Colizza, A. Barrat, M. Barthlemy, and A. Vespignani, *PNAS*. **103**, 2015 (2006).
- [44] M. Kuperman and G. Abramson, *Phys. Rev. Lett.* **86**, 2909 (2001).
- [45] M. Wardetzky, S. Mathur, F. Kälberer, and E. Grinspun, in *Proceedings of the fifth Eurographics symposium on Geometry processing* (Eurographics Association, 2007) pp. 33–37.
- [46] K. M. Page, P. K. Maini, and N. A. M. Monk, *Physica D: Nonlinear Phenomena* **202**, 95 (2005).
- [47] A. V. Chechkin, R. Gorenflo, and I. M. Sokolov, *J. Phys. A* **38**, L679 (2005).
- [48] C. Angstmann and B. I. Henry, *Phys. Rev. E* **84**, 061146 (2011).
- [49] A. N. Samukhin, S. N. Dorogovtsev, and J. F. F. Mendes, *Phys. Rev. E* **77**, 036115 (2008).
- [50] G. Xu, *CAGD* **21**, 767 (2004).
- [51] R. G. Plaza, F. Sánchez-Garduno, P. Padilla, R. A. Barrio, and P. K. Maini, *J. Dyn. Differ.*

Equ. **16**, 1093 (2004).

[52] J. D. Murray, *Mathematical biology*, Vol. 2 (Springer, 2002).

[53] D. J. Watts and S. H. Strogatz, *Nature* **393**, 440 (1998).

[54] P. F. Verhulst, *Mémoires de l'Académie Royale des Sciences et des Belles-Lettres de Bruxelles* **18**, 1 (1845).